J Mater Sci: Mater Electron (2008) 19:577–583
DOI 10.1007/s10854-007-9392-4

Phase formation and microstructure of Nd^{+3} doped $Pb(Mg_{1/3}Nb_{2/3})O_3$ prepared by sol–gel method

Aylin Şakar-Deliormanlı · Erdal Çelik · Mehmet Polat

Received: 14 April 2007 / Accepted: 27 August 2007 / Published online: 10 October 2007

Abstract The aim of this study was to investigate the effects of the rare earth element neodymium on the phase formation and microstructural development of relaxor ferroelectric lead magnesium niobate, $Pb(Mg_{1/3}Nb_{2/3})O_3$ (PMN) system. Perovskite phase PMN powders were prepared using the sol–gel method and the effect of neodymium doping was investigated at different doping levels ranging from 0.1 mol% to 30 mol%. The precursors employed in the sol–gel process were lead (II) acetate, magnesium ethoxide, and niobium (V) ethoxide. All the experiments were performed at room temperature while the calcination temperatures ranged between 800 °C and 1,100 °C. Results showed that it was possible to obtain the pure perovskite phase at 950 °C using the sol–gel method. Nd^{+3} addition influenced the phase formation and microstructure of the multicomponent system. Pyrochlore was detected along with the perovskite phase above 10 mol% Nd. Results also demonstrated that grain size of the synthesized powders depended on the Nd^{+3} concentration.

1 Introduction

Lead magnesium niobate (PMN) is a relaxor ferroelectric material that is characterized by a diffuse phase transition over a broad temperature range and a frequency dependent maximum in its relative dielectric permittivity. It demonstrates very high dielectric constant around –10 to –5 °C [1]. It has many potential applications such as multilayer ceramic capacitors, actuators and electro-optic devices [2].

In the processing of PMN ceramics, synthesis of pure perovskite phase is crucial, the most important problem being the formation of pyrochlore phase which degrades the electrical properties. Previously, several attempts have been made to eliminate the pyrochlore in the PMN structure. The Columbite method introduced by Swartz and Shrout, addition of excess MgO to promote the perovskite formation, and excess PbO addition to compensate lead oxide evaporation during calcination are the commonly used techniques to prevent pyrochlore formation [3–5].

Among others, the sol–gel method offers several advantages for the preparation of ceramic oxides. This method provides high degree of homogeneity and stoichiometry especially for multicomponent systems in addition to allowing doping on a molecular scale. Hence, there is considerable interest in the preparation of PMN ceramics using sol–gel method [6–11].

The phase formation and electrical properties of piezoelectric ceramics can be modified by use of dopants. Effects of rare earth elements (RE) doping on the phase formation and electrical properties of piezoelectric ceramics such as barium titanate and lead zirconate titanate are well studied [12–15]. The effect of RE addition on the PMN system has also been studied in the literature to a degree. Zhong et al. [16] studied the effects of adding a fixed amount of rare earth additives on the microstructure and dielectric properties of PMN-PT ceramics. Their results showed that doping of neodymium (Nd^{+3}) resulted in a slight decrease in the grain size and a lowering of the dielectric constant [16]. Kim et al. [17] and Branileau et al. [2] studied effect of lanthanum (La^{+3}) additions on the

A. Şakar-Deliormanlı (✉) · M. Polat
Chemical Engineering Department, Izmir Institute of Technology, Urla, Izmir 35430, Turkey
e-mail: aylindeliormanli@iyte.edu.tr

E. Çelik
Metallurgy and Materials Engineering Department, Dokuz Eylül University, Izmir, Turkey

phase formation of PMN ceramics. The former study indicated that the presence of La^{+3} cations implied an increase in the short range ordering, resulting negative space-charge balance into the ordered domains in PMN [3].

In the majority of these previous studies it is observed that the effects of RE addition has been studied using solid state reactions and at fixed RE compositions. Also, no published work on the effect of Nd^{+3} doping in the PMN system is encountered. Therefore, the aim of the present work is to examine the phase formation and microstructural evolution in neodymium-modified lead magnesium niobate powders prepared by the sol–gel method.

2 Experimental

2.1 Materials

Starting materials for the sol–gel synthesis were lead (II) acetate trihydrate, [$Pb(CH_3COO)_2 \cdot 3H_2O$, 99.5%, Riedel-de Haen), magnesium ethoxide, [$(C_2H_5O)_2Mg$, 95%, Aldrich], and the niobium ethoxide [$Nb(OC_2H_5)_5$, 99.999%, Alfa Aesar]. Neodymium (III) acetate hydrate [$(CH_3COO)_3 \cdot Nd \cdot xH_2O$, 99.9%, Aldrich] were the precursor used for the preparation of the Nd-doped lead magnesium niobate samples. Ethylene glycol [$C_2H_6O_2$, >99.5%, Merck], and methanol [CH_3OH, 99.7%, Riedel-de Haen] were utilized as the solvents to prepare the solutions. Glacial acetic acid [99.5%, Panreac Quimica SA] was used as the additive for the molecular reactions with alkoxides.

2.2 Powder synthesis

For powder synthesis, 3.81 g Pb–acetate was dissolved in 10 mL solvent (methanol or ethylene glycol) and 2 mL acetic acid until complete dissolution which was accomplished within few minutes. If the sample was to be doped, neodymium acetate was added to this solution at this stage. However, the solubility of the neodymium acetate was very low under this condition. Subsequently, a 0.388 g sample of magnesium ethoxide was added along with additional 10 mL methanol and acetic acid. Addition of the magnesium ethoxide accelerated the dissolution of the Nd acetate. The solution was stirred continuously until the complete dissolution of the precursors. Finally, a 1.67 mL aliquot of Nb–ethoxide, which was already cooled down to 5 °C, was added to the main suspension, resulting in a transparent solution which turned opaque lilac with time. The solution was hydrolyzed at a hydrolysis ratio of 3 and kept at room temperature for curing. Complete gelation occurred within 1 day if the solvent was methanol. More homogeneous and strongly bonded gel network was obtained in the case of Nd^{+3} doped samples compared to undoped species. Gels were initially dried at room temperature followed by drying at 80 °C.

Calcination of the samples was performed in air at 500 °C at a heating rate of 10 °C/min for 3 h to ensure the total removal of organic materials. These samples were then heated to various temperatures, namely 800, 900, 950, and 1,100 °C at a heating rate of 5 °C/min and were kept at these temperatures for 2–8 h. During heat treatment, double alumina crucible system with cover was used in order to prevent the lead loss from the samples. To provide a lead rich atmosphere lead zirconate ($PbZrO_3$) powder was used in the outer crucible. The general experimental scheme for the PMN powder synthesis is shown in Fig. 1.

In the case of Nd^{+3} doping, the Nd^{+3} concentration (x) in samples was varied between 0.001 and 0.30. When the samples were doped with Nd^{+3}, it was necessary to account for the charge imbalance. One way was to keep the ratio of Mg:Nb concentration fixed which would result in the A site vacancies $Pb_{1-3x/2}\ Nd_x\ (Mg_{1/3}Nb_{2/3})O_3$ [18]. However, in this study, Mg:Nb ratio was increased in order to balance the donor charge of Nd^{+3} and to prevent A site vacancies. Hence, the compositions were expressed by the following formula $Pb_{1-x}Nd_x\ (Mg_{(1+x)/3}\ Nb_{(2-x)/3})O_3$.

2.3 Characterizations

Thermal properties were examined using a Thermogravimetric analyzer (TGA-51/51 H from Shimadzu, Japan) up to 500 °C at a heating rate of 20 °C/min under nitrogen

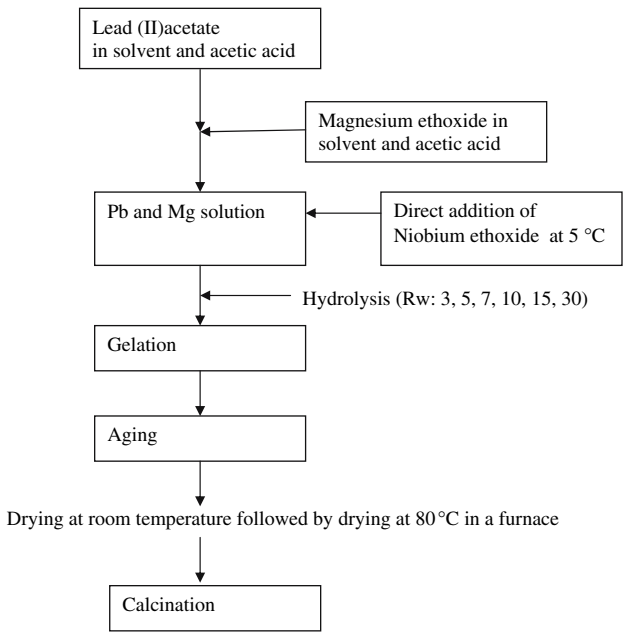

Fig. 1 General scheme showing the powder preparation steps

atmosphere. The infrared spectra of the powders were obtained using Fourier Transform Infrared Spectroscopy (FTIR-8201 from Shimadzu, Japan). Microstructures were observed by Scanning Electron Microscope (JSM-6060 JEOL). The powders were dry ground using an agate mortar and pressed into disks (15 mm in diameter and 2 mm thick) using a hydraulic press prior to SEM analysis. Phase evolution of the samples were studied by X-ray diffractometer (Philips, X'Pert Pro) using CuKα radiation.

Relative amounts of perovskite and pyrochlore phase were determined using the following approximation equation:

$$\%\text{pyrochlore} = \frac{I_{\text{pyro}}}{I_{\text{pyro}} + I_{\text{perovskite}}} \times 100$$

where I_{pyro} and $I_{\text{perovskite}}$ are the intensities of the major peaks of the pyrochlore (222) and perovskite (110) phases [19].

3 Results and discussion

3.1 Phase analysis by X-ray diffraction

3.1.1 Effect of calcination temperature

Figure 2 represents the XRD diagrams of the PMN powder samples calcined at different temperatures. It can be seen from Fig. 2-a that crystallization already takes place at 500 °C with the formation of the pyrochlore phase. Further heating to a higher temperature initiates the perovskite phase and a very rich perovskite structure is achieved at 800 °C even though traces of pyrochlore can be identified (Fig. 2-b). The perovskite content was determined around 90.8% under this condition. Still further heating to 950 and 1,100 °C results in pure perovskite phase (Fig. 2-c, d).

3.1.2 Effect of solvent type

It is well known that alkoxide reactivity can be easily modified by changing the solvent which affects the gelation rate along with the properties of the oxide [20]. In the present study, ethylene glycol was the first solvent tested since it was expected to inhibit the very high hydrolysis rate of Nb-ethoxide. However, it was observed that the solutions prepared by ethylene glycol rarely constituted gelation even at temperatures above 25 °C. The gelation was less than satisfactory when this solvent was used. Hence, methanol was tested as the other solvent in our multicomponent system. Beltran et al. observed a white precipitate on the addition of niobium ethoxide to methanol which may caused by the hydrolysis of the Nb(V) ions [6]. However, in our experiments precursor materials Pb–acetate, Mg–ethoxide, and Nb–ethoxide were easily dissolved in methanol at room temperature and formed a transparent solution. Figure 2a–c describes the diffraction patterns of the

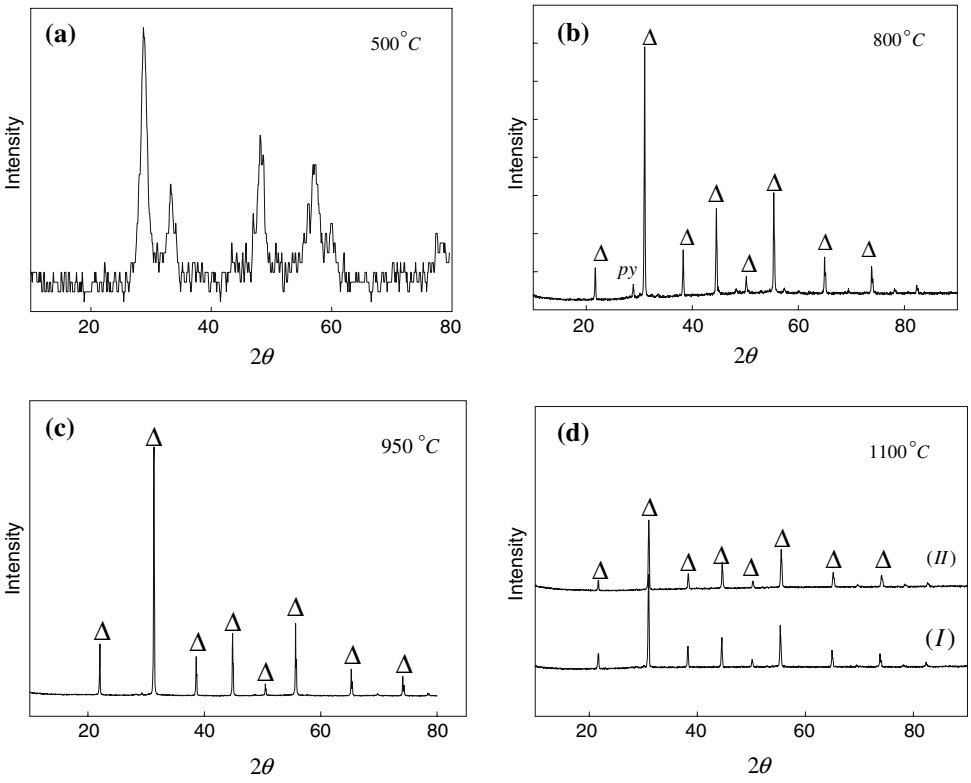

Fig. 2 PMN samples calcined at (**a**) 500 °C for 3 h (**b**) 800 °C for 8 h (**c**) 950 °C for 2 h (**d**) 1,100 °C for 2 h (I) solvent: methanol (II) solvent: ethylene glycol. (Δ) perovskite (py) pyrochlore

samples prepared using methanol. Similarly, Figure 2-d shows the XRD patterns of the powders prepared using ethylene glycol and methanol. Although XRD patterns of the powders prepared using both solvents indicates the formation of perovskite phase, peak intensities are slightly higher for the case of methanol.

3.1.3 Effect of hydrolysis ratio

In the sol–gel process the reactions can be attributed to the hydrolysis of the precursor, leading to the formation of M–OH bonds, followed by a polycondensation process with the departure of water or an alcohol molecule [21]. The effect of hydrolysis ratio (Rw) on the perovskite phase formation can be observed in Fig. 3. Results showed that intensities of the diffraction patterns are lower at high water gels (Rw 15 and 30). It is important to note that diffraction patterns were collected using the same collection times and instrumental conditions. Therefore, intensity differences were attributed to the difference in phase formation mechanism depending on the hydrolysis ratio.

Similarly, previous study of Lakeman and Payne showed that in PZT gels all reactions were completed at lower temperature in low water gels (Rw: 2.0 and 3.0) whereas high water gels (Rw: 10) displayed more diffuse behavior with several peaks and required higher temperature to complete the reaction [22, 23]. It is possible to correlate this behavior with the formation and the development of the perovskite phase.

3.1.4 Effect of neodymium doping

The XRD patterns presented in Figs. 4 and 5 demonstrate the effect of Nd^{+3} doping on the phase formation as a function of Nd^{+3} concentration. It is clear that at high concentrations (above 10 mol%) Nd^{+3} causes the formation of unwanted pyrochlore phase. In the composition pyrochlore amounts were calculated to be 9.1% and 6.6% in the presence of 30 and 20 mol% Nd^{+3}, respectively.

According to the results of Majumder et al. [14] who studied the effect of Nd^{+3} on the PZT thin films, a pure perovskite phase was obtainable up to 5 wt% and a pyrohlore phase was found to coexist with perovskite structure beyond this concentration [14]. In the current study Figs. 4 and 5 reveal that intensity of the perovskite phase peaks are slightly higher for the sample that contains 0.5 mol% Nd compared to the undoped sample. Furthermore, Nd^{+3} doping between 0.1 mol% and 7 mol% did not cause the pyrochlore formation. However, the detrimental effect observed beyond 10 mol%.

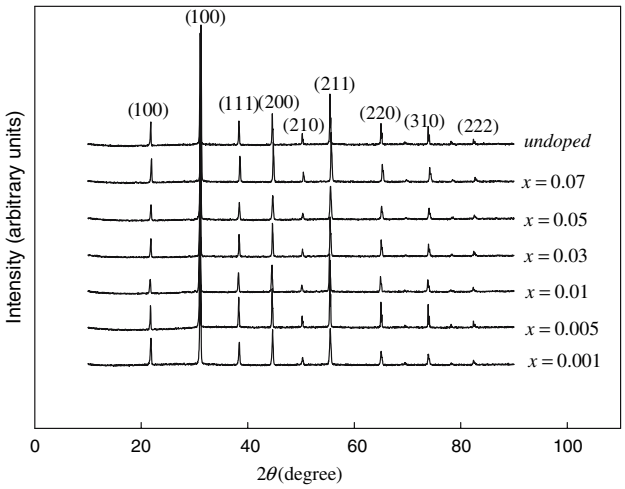

Fig. 4 XRD diagrams of the undoped and Nd-doped PMN samples at different Nd concentrations. Calcination at 1,100 °C for 2 h

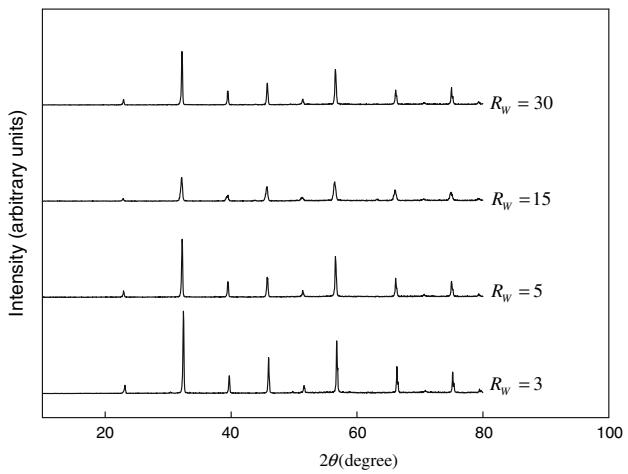

Fig. 3 XRD diagrams of the PMN powders prepared by different hydrolysis ratios. Calcination at 1,100 °C for 2 h

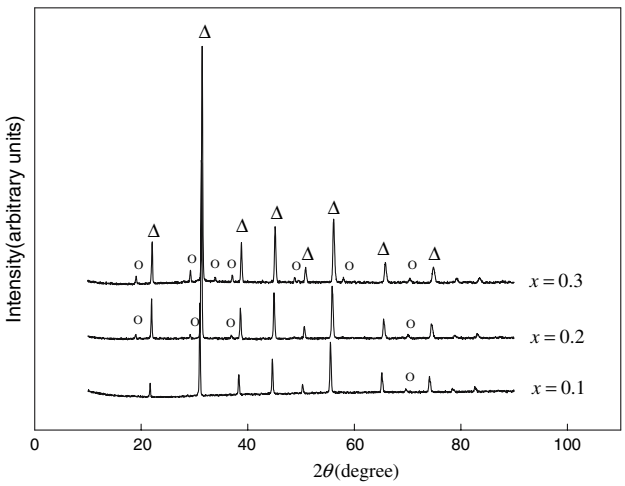

Fig. 5 XRD diagrams of the Nd-doped (10, 20, 30 mol%) PMN samples. Calcination at 1100 °C for 2 h (Δ) perovskite, (°) pyrochlore

3.2 TGA and FTIR analyses

Figure 6 presents the TGA analysis of the dried PMN gel. The TGA profile displays that the weight loss initiates at about 260 °C and continuous until 400 °C at which organic phases have been completely removed. From this temperature on the weight of the sample remains constant. The weight losses observed in the figure were attributed to the dehydration and subsequent elimination of the organic components.

FTIR analysis of the PMN and Nd-doped PMN samples were carried out on dried powders along with those samples calcined at different temperatures. The results are presented in Fig. 7. The presence of organics in dried powders is indicated by two sharp peaks at wavelengths 1,300–1,400 cm^{-1} and 1,600–1,700 cm^{-1} which corresponds to C–O and C=C stretching vibrations, respectively. A similar band at 1,700 cm^{-1} characterizes the valence vibrations of –C=O group in acetic acid and its esters. The vibrational band over the range of 3,200–3,700 cm^{-1} indicates the –OH groups in the sample. Upon heating the band intensities relating to both

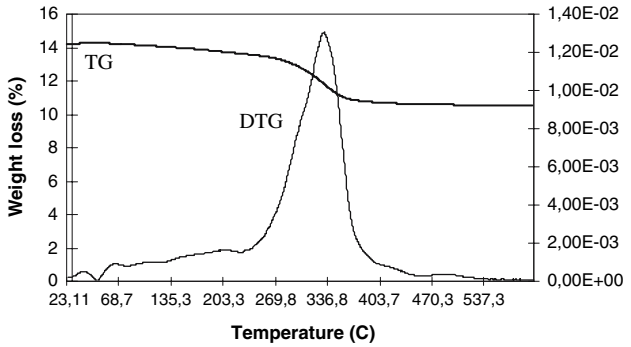

Fig. 6 TGA and derivative-TGA profile of the PMN gel

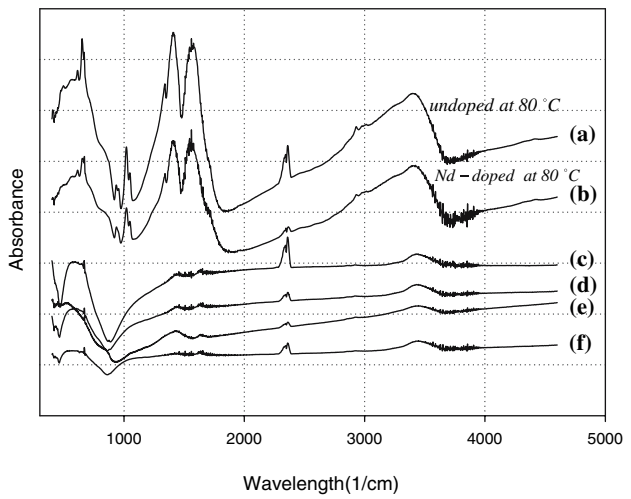

Fig. 7 FT-IR spectra of the PMN and Nd-doped PMN powders (a) undoped sample dried at 80 °C (b) 20 mol% Nd-doped PMN, dried at 80 °C (c) Nd-doped PMN, at 1,100 °C (d) PMN at 500 °C (e) PMN at 900 °C (f) PMN at 1,100 °C

hydroxyl and organic groups are reduced. However, these bands are still visible even for the samples calcined at 1,100 °C. The band around 500–900 cm^{-1} corresponds to the metal oxygen bonds [22, 24].

3.3 Microstructural evolution

The experimental work demonstrated that control of the particle size distribution was very difficult owing to the rapid hydrolysis rate of metal alkoxides and that the morphology of the products depended on the neodymium concentration in the structure. The SEM micrographs of the selected samples are presented in Fig. 8 to demonstrate the effect of Nd^{+3} doping and calcination temperature on the grain size. It can be seen in Fig. 8-a that grain size of the undoped sample calcined at 1,100 °C is greater than 1 micron. Surface area (BET) of the same powder is less than 10 m^2/g, which confirms the rather coarse particle size. However, the grain size is much smaller (average 350 nm) for the PMN powder calcined at 800 °C (See Fig. 8-b).

When an additive oxide is added to the perovskite structure (ABO_3), the added cation distributes itself between the A and B sites in a ratio which depends upon the ionic radius and valance of the cation. Considering the radii of ions in our doped PMN system (1.20, 0.74, 0.69, and 0.995 Å for Pb^{+2}, Mg^{+2}, Nb^{+5}, Nd^{+3} respectively), it is reasonable to expect that Nd^{+3} should preferentially occupy the Pb^{+2} lattice [8]. The results given in Fig. 8-c–g shows that the doping of Nd^{+3} in the range of 3–10 mol% clearly causes an increase in the grain size. However, it is interesting to note that at higher Nd^{+3} concentrations the trend is reversed and the grain size is reduced. In a previous research Braileanu et al. [2] observed a decrease in the grain size of 2 mol% lanthanium-doped PMN samples from 8 μm to 5 μm. They interpreted their observations such that using La^{+3} based admixture determines the incorporation of the La^{+3} on the Pb^{+2} site acting as the donor dopant [2]. Similarly, Kim et al. [17] reported that La-doping at <1 mol% resulted in the decrease in the grain size of PMN and PMN-PT ceramics. The behavior was explained by solid-solution impurity drag mechanism [17].

Another model implies that La^{+3} ions concentrate in greater amounts on grain boundaries than that inside the bulk of the grains. Hence, La^{+3} reacts with such defects as pyrochlore or lead and oxygen vacancies within the grains which leads to the observed reduction in grain growth [16]. Still yet, Zhong et al. [16] showed that doping of Nd^{+3} resulted in slight decrease in grain sizes of the PMN-PT powders [16]. Another possible explanation for the decrease in the grain size of the PMN powders is the formation of the pyrochlore phase. Costa et al. [19] showed that presence of a few percentage of pyrohlore phase

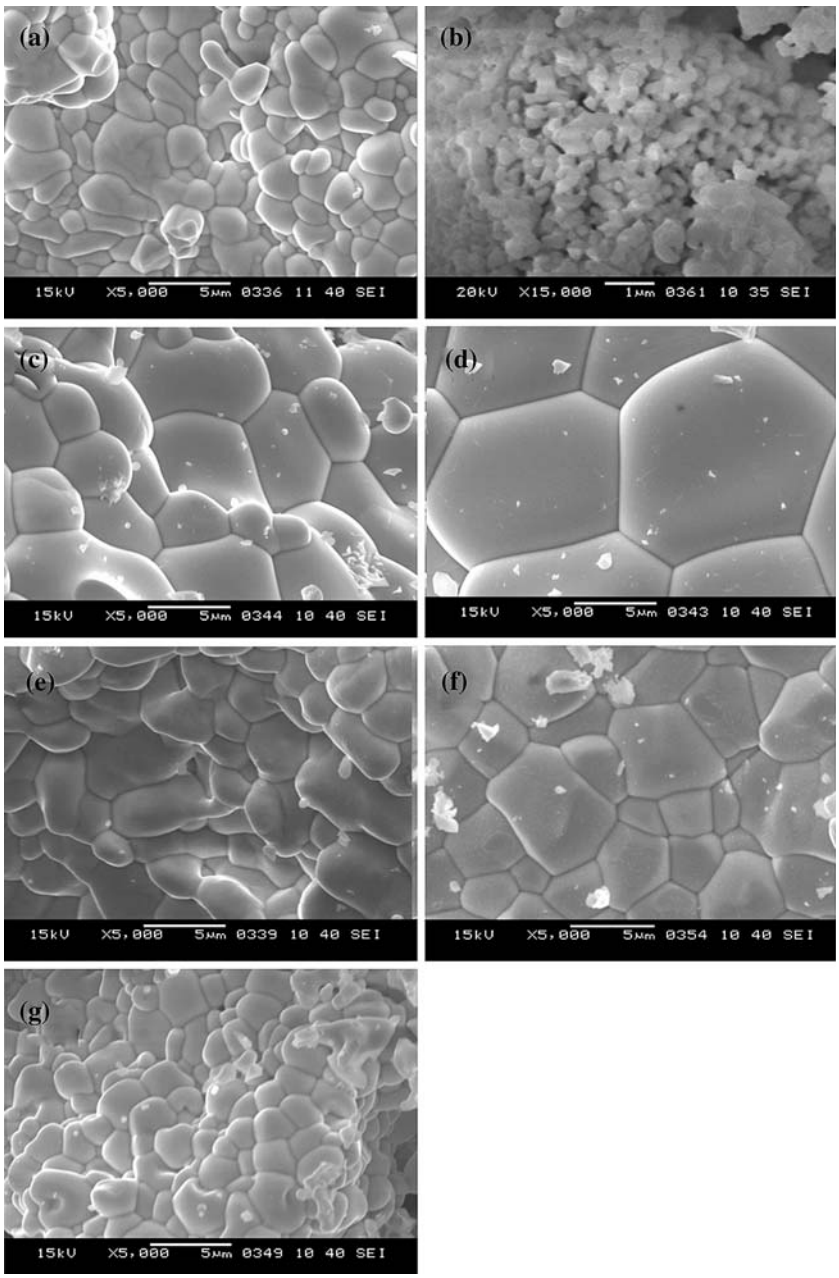

Fig. 8 SEM micrographs of PMN and Nd-doped PMN at different Nd concentrations. Natural surface (**a**) undoped sample calcined at 1,100 °C (**b**) undoped sample calcined at 800 °C (**c**) Nd-doped, $x = 0.03$ (**d**) Nd-doped, $x = 0.05$ (**e**) Nd-doped, $x = 0.07$ (**f**) Nd-doped, $x = 0.1$ (**g**) Nd-doped, $x = 0.2$. All doped samples calcined at 1,100 °C for 2 h

lowers the grain sizes and the dielectric constant of the PMN system [19].

On the other hand, the space-charge model may also give a possible explanation for the grain growth mechanism of the doped PMN samples. According to this model, ordered regions in PMN are Mg^{+2} rich and carry a net negative charge whereas the matrix surrounding the ordered regions is Nb^{+5} rich and carries an equal positive charge. Therefore, it is reasonable to state that the strong charge effects and the ordered domains within this structure can be effective to inhibit the grain growth. In addition, donor doping in the A site, such as lanthanum or neodymium, should facilate the growth of the ordered domains because of the compensation of the charge imbalance [25].

4 Conclusions

Perovskite PMN powders were synthesized using a straight forward sol–gel method at room temperature. Hydrolysis conditions as the hydrolysis ratio were observed to influence the phase formation. Pyrochlore free structures were obtained by calcination at 950 °C for 2 h in a lead-rich atmosphere.

Substitution of neodymium to the PMN lattice influenced the morphology of the synthesized powders. Grain size increased drastically after 5 mol% Nd^{+3} doping whereas a decrease in the grain size was observed at higher Nd^{+3} concentrations. At concentrations higher than 10 mol% of Nd^{+3}, a pyrochlore phase was observed to coexist with the perovskite phase.

Acknowledgments The financial support by the Izmir Institute of Technology and The Scientific and Technological Research Council of Turkey is gratefully acknowledged. The authors would like to thank Izmir Institute of Technology, Material Research Center for use of the XRD.

References

1. S. Fengbing, L. Qiang, Z. Haisheng, L. Chunhong, Z. Shixi, S. Dezhong, Mater. Chem. Phys. **83**, 135 (2004)
2. A. Brailenau, A. Ianculescu, M. Zaharescu, I. Pasuk, S. Preda, J. Madarasz, G. Pokol, Key Eng. Mater. **1309**, 264–268 (2004)
3. V.V. Bhat, B. Angadi, A.M. Umarji, Mater. Sci. Eng. B. **131**, 116 (2005)
4. S. Ananta, T.W. Noel, J. Eur. Ceram. Soc. **19**, 629 (1999)
5. S.L. Swartz, T.R. Shrout, Mat. Res. Bull. **17**, 1245 (1982)
6. H. Beltran, E. Cordoncillo, P. Escribano, J.B. Carda, A. Coats, A.R. West, Chem. Mater. **12**, 400 (2000)
7. H. Beltran, N. Maso, B. Julian, E. Cordoncillo, B.J. Carda, P. Escribano, J. Sol–Gel Sci. Tech. **26**, 1061 (2003)
8. K. Babooram, H. Tailor, Z.G. Ye, Ceram. Int. **30**, 1411 (2004)
9. F.A.-W. Su, Mater. Chem. Phys. **62**, 18 (2000)
10. S. Komerneni, R.I. Abothu, A.V. Prasada Rao, J. Sol–Gel Sci. Tech. **15**, 263 (1999)
11. Z. Jiwei, S. Bo, Z. Liangying, Y. Xi, Mater. Chem. Phys. **64**, 1 (2000)
12. J. Singh, N.C. Soni, S.L. Srivastava, Bull. Mater. Sci. **26**, 397 (2003)
13. A. Garg, D.C. Agraval, Mater. Sci. Eng. B. **86**, 134 (2001)
14. S.B. Majumder, B. Roy, R.S. Katiyar, S.B. Krupanidhi, J. Appl. Phys. **90**, 2975 (2001)
15. H Kishi, N. Kohzu, J. Sugino, H. Ohsato, Y. Iguchi, T. Okuda, J. Eur. Ceram. Soc. **19**, 1043 (1999)
16. N. Zhong, P.-H. Xiang, D.-Z. Sun, X.-I. Dong, Mater. Sci. Eng. B. **116**, 140 (2005)
17. N. Kim, S.J. Jang, T.R. Shrout, in *Proceedings of the 1990 IEEE International Symposium on Applications of Ferroelectrics*, 1991, pp. 605–609
18. D.M. Fanning, I.K. Robinson, S.T. Jung, E.V. Colla, D.D. Viehland, D.A. Payne, J. Appl. Phys. **87**, 840 (2000)
19. A.L. Costa, C. Galassi, G. Fabri, E. Roncari, C. Capiani, J. Eur. Ceram. Soc. **21**, 1165 (2001)
20. T. Fukui, C. Sakura, M. Okuyama, J. Mater. Sci. **32**, 189 (1997)
21. H. Brunckova, L. Medvecky, J. Briancin, K. Saksl, Ceram. Int. **30**, 453 (2004)
22. T.H. Lee, I.W. Lee, H.Y. Kim, C.M. Whang, Kor. Ceram. Soc. Bull. **23**, 1078 (2002)
23. C.D.E. Lakeman, D.A. Payne, J. Am. Ceram. Soc. **75**, 3091 (1992)
24. W. Beng Ng, J. Wang, S. Choon Ng, L.M. Gan, J. Am. Ceram. Soc. **82**, 529 (1999)
25. S. Miao, X. Zhang, J. Zhu, J. Am. Ceram. Soc. **84**, 2091 (2001)